

# Fatigue behaviour of some temperature-resistant polymers

J. P. TROTIGNON, J. VERDU

*ENSAM, 151 bd de l' Hôpital, 75013 Paris, France*

CH. MARTIN, E. MOREL

*IRCHA ou SNPE, B.P. 1, 91710 Vert le Petit, France*

Static and flexural (5 Hz, 20 °C) fatigue properties of three linear polymers, polyetherimide (PEI), polysulphone (PSU), polyetheretherketone (PEEK) and one three-dimensional polymer, amine cross-linked epoxy (EPO), were compared. In all cases, the fatigue lifetime was governed by crack initiation and a brittle rupture occurred. The order of stress endurance limit is: PEEK (65 MPa) > EPO (28 MPa) > PEI (24 MPa) > PSU (18 MPa). For PEI and essentially PSU, this value increased with orientation. It thus appears that there is no relation between the fatigue durability and the ductility or toughness as established from static tests. The results suggest that crack initiation involves large-scale configurational changes such as crazing. These changes would be inhibited or reduced by chemical (EPO) or physical (semi-crystalline polymers such as PEEK), cross-linking.

## 1. Introduction

The cyclic fatigue of polymeric materials can often be described as a two-stage phenomenon (at least for unnotched samples). During the first stage, which can be called the induction or initiation stage (IS), the stress-induced structural changes (which could, for instance, be described in terms of submicrodefects [1]), have no significant influence on the sample macroscopic compliance. In a test at a fixed amplitude of deformation, the induced stress becomes constant as soon as the thermal equilibrium is reached. The second (and final) stage can be termed the crack-propagation stage (CPS). Its onset corresponds to the coalescence of microdefects to form cracks capable of propagation. It can be experimentally detected by the resulting decrease of modulus, i.e. a decrease in the induced stress in a test made at fixed amplitude of deformation.

A large amount of literature is available on the experimental study of the fatigue of notched specimens [2–5]. Indeed, the initiation stage is suppressed in this case, and the sample lifetime is only controlled by its resistance to crack propagation, whose kinetics can be analysed in terms of fracture mechanics. Here, it seems possible to predict the long-term behaviour from short-term measurements of characteristics, such as the stress intensity factor,  $K_{Ic}$  [6].

In many cases of unnotched specimens, however, the duration of the CPS (until sample breakdown) appears as a very low fraction of the overall fatigue lifetime which is essentially controlled by the initiation rate. The structure-properties relationships do not seem to be clearly established in this case.

For semi-crystalline polymers, complications can

result because of the fact that the fatigue behaviour depends on their morphology which, in turn, depends in a complex way on the processing conditions, as shown in the case of polypropylene [7]. It appears, however, that semi-crystalline polymers such as polyamides [6, 8], polyvinylidene fluoride (PVDF) [6, 8], PEEK [8] or polyphenyl sulphide (PPS) [8] are generally more fatigue resistant than amorphous polymers of comparable static characteristics.

For amorphous glassy polymers, relatively little is known on the structural factors governing the fatigue durability. Very interesting observations have been made, however, on a very specific cracking pattern termed the “epsilon crack-tip plastic zone” which appears, for instance, in polycarbonate [9] or in PPS [10]. Undulating tension tests made on 12 glassy polymers showed that this pattern is favoured when shear flow is competitive relative to crazing or breakdown, which can be expressed by the ratio  $\epsilon_c/\sigma_y$ ,  $\epsilon_c$  being the critical strain for crazing and  $\sigma_y$  the yield stress.

Another interesting feature of certain glassy polymers such as polycarbonate [11] is their very high notch-sensitivity despite their relatively high ductility and toughness.

In the present work, a peculiar attention was paid to the duration of the initiation stage and to the stress endurance limit (SEL) for various polymers having a relatively high heat-deflection temperature: polysulphone (PSU), polyetherimide (PEI), polyetheretherketone (PEEK) and amine cross-linked epoxy (EPO). They have been compared with polymers of lower performance, for instance polypropylene (PP) polyamide (PA) or polycarbonate (PC) fatigue tested under the same conditions.

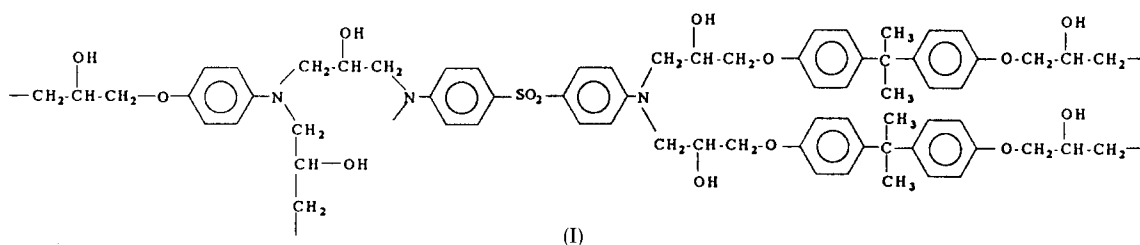


TABLE I Injection-moulding conditions for both linear polymers under study

Polymers	Compression Moulding temperature °C	Injection conditions			
		Nozzle temperature °C	Injection pressure (MPa)	Injection rate (mm s <sup>-1</sup> )	Mould temperature °C
PSU	305	390	11	5	120
PEI	300	330	20	15	90
PEEK	—	400	100	25	170

## 2. Experimental procedure

### 2.1. Materials

PEI, PSU and PEEK are industrial polymers of respective trade names: ULTEM 1000 (General Electric Plastics), UDEL P. 1700 (Union Carbide), VICTREX (ICI). EPO is a laboratory-made network based on a 50/50 (by weight) mixture of two epoxides: diglycidylether of bisphenol A (DGEBA), and triglycidyl amino phenol (TGAP), cross-linked by a stoichiometric amount of diaminodiphenyl sulphone (DDS). The network structure can be tentatively represented as shown in (I). It was cured 3 h at 130 °C plus 3 h at 180 °C. Under these conditions, no residual exotherm appeared in the differential scanning calorimetry (DSC) scans.

### 2.2. Sample preparation

EPO samples for mechanical testing were cut from the moulded blocks with a diamond saw. Their ridges were polished in order to minimize roughness effects on fatigue and static testing [12]. For glassy polymers PEI and PSU, two methods were used.

(i) Compression moulding at 3 MPa for 3 h. The samples were machined from the moulded plaques in order to obtain ISO type 1 tensile test specimens according to the French Standard AFNOR NFT 51034.

(ii) Injection moulding in a mould cavity corresponding to the above standard, with a single injection gate located in a sample head. The samples were quenched, in order to minimize orientation relaxation, in cold water (PSU) or in air (PEI). Samples were also prepared with different holding pressures (9 or 4 MPa).

Some processing parameters are listed in Table I. In the case of PEEK, only injection moulding was used. The processing parameters are also listed in Table I. The sample thickness was 4 mm in all cases.

### 2.3. Fatigue testing

A previously described universal machine [13] was used for fatigue testing at 5 Hz, 20 °C, and constant

amplitude of deformation with a continuous recording of the induced stress.

Two loading modes, alternate bending mode (ABM) and undulating bending mode (UBM), were studied. Both cases correspond to a sinusoidal waveform but the first one (ABM) is symmetric (zero average stress), whereas the second one (UBM) is asymmetric, the minimal stress being 10% of the maximum stress, unless specified. Both loading modes are shown schematically in Fig. 1.

In the case of ABM, tensile samples were used and the most strained zone was always the same, taking into account that single-gated injection-moulded parts are not morphologically symmetrical. In the case of UBM, parallelepipedic bars were used, the span distance being 100 mm.

### 2.4. Static testing

Thermophysical and tensile properties were determined by the classical methods. For the glassy polymers PEI, PSU and EPO, ultrasonic moduli were determined at 20 °C, 5 MHz, and the packing densities ( $\rho^* = \text{Van der Waals volume/total volume}$ ), were calculated according to previously published methods [14].

The fracture mechanics characteristics,  $K_{Ic}$  and  $G_{Ic}$ , were determined from crack propagation-rate measurements made at 20 °C,  $1.6 \times 10^{-4} \text{ s}^{-1}$  strain rate on classic double Cantilever specimens.

## 3. Results

### 3.1. Physical properties

The results of measurements of some physical properties are summarized in Table II.

EPO appears to be more densely packed than the amorphous phase of the linear polymers, which results essentially from hydrogen bonding [15]. This also explains the especially high ultrasonic modulus of EPO [14]. The glass transition temperatures of glassy polymers are relatively close ( $493 \pm 15 \text{ K}$ ). The corresponding damping peak in viscoelastic spectra is

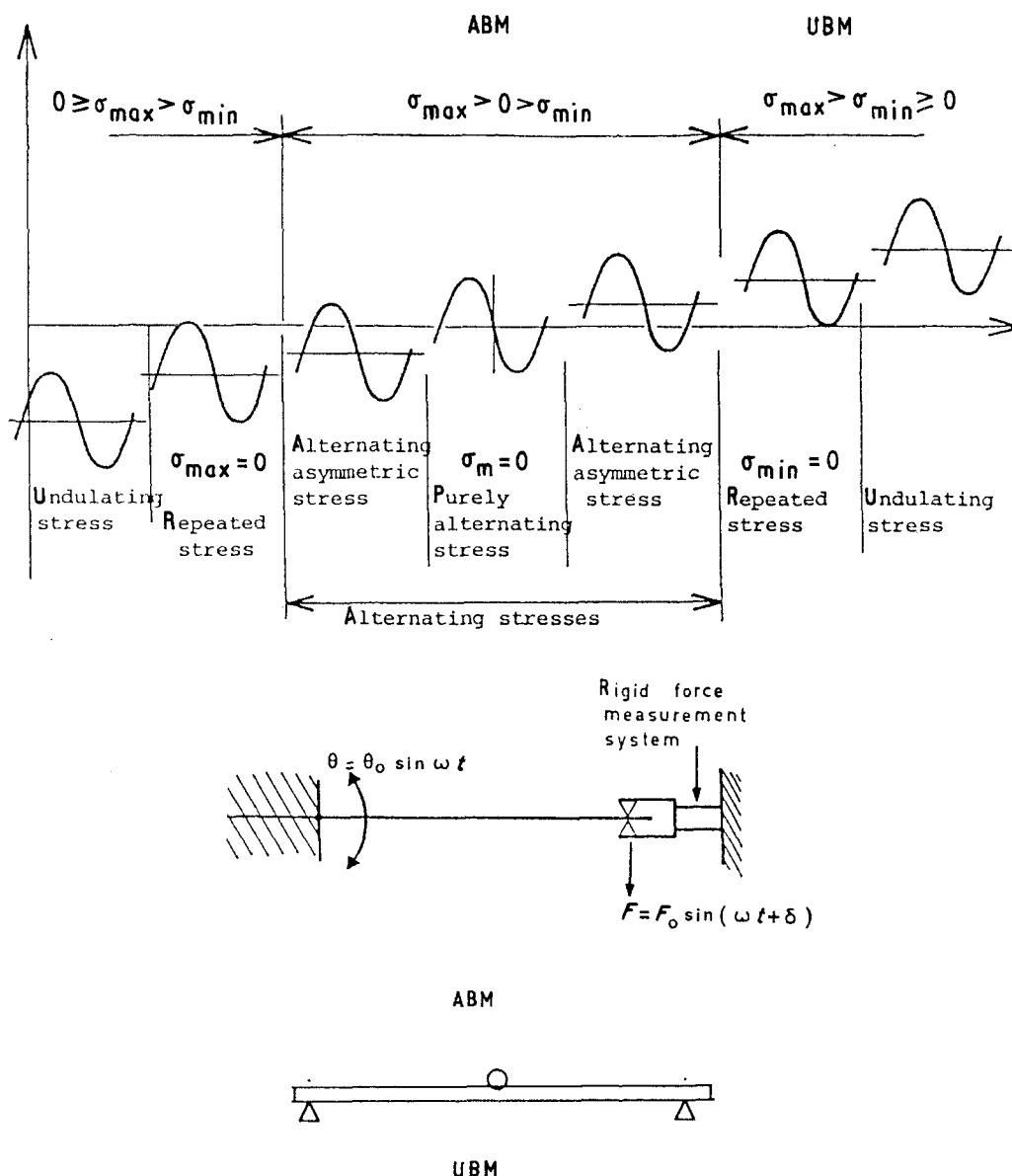


Figure 1 Schematic diagram of the two fatigue loading modes (see text) and the corresponding stress variations.

TABLE II Physical properties of the polymers under study

	EPO	PEI	PSU	PEEK
Tensile modulus, $E_t$ (GPa)	3.04	3.0	2.5	3.6
Ultimate stress, $\sigma_r$ (MPa)	97	90	70	92
Ultimate elongation, $\epsilon_r$ (%)	4.7	60	100	50
$K_{Ic}$ (MPa m <sup>1/2</sup> )	0.63	2.93	3.54	6
$G_{Ic}$ (J m <sup>-2</sup> )	114	2042	5000	10000

<sup>a</sup> See text.

<sup>b</sup> Measured by DMTA at 0.33 Hz.

<sup>c</sup> Determined at 5 MHz, 20°C.

<sup>d</sup> Calculated assuming a complete conversion of the epoxide-amine reaction.

<sup>e</sup> Determined for the amorphous phase.

smaller and wider for EPO than for PSU and PEI. This peak widening could be attributed to some morphological heterogeneity; however, a previous study [16] showed that in epoxies of this type, the fracture properties are essentially governed by the molecular structure.

### 3.2. Static mechanical properties

Some static properties are summarized in Table III. The polymers are considerably more ductile and tough than the network (EPO) under study.

The Young's moduli are of the same order of magnitude,  $E \approx 3.0 \pm 0.6$  GPa, which will make further comparisons of the fatigue behaviour relatively easy. The order of stiffness values, PEEK > EPO and PEI > PSU, can be explained by the combination of the well-known effects of crystallinity (PEEK), cohesion (EPO > linear polymers) and local mobility in the amorphous phase (EPO < linear polymers).

### 3.3. Fatigue properties

#### 3.3.1. General aspects

All the stress-number of cycles ( $SN$ ) curves have the shape of Fig. 2. The stress remains constant over more than 95% of the time to rupture, so that the length of the IS plateau, expressed in terms of number of cycles,  $N_r$ , can be assimilated to the fatigue lifetime. The corresponding stress amplitude,  $S$ , is indeed an increasing function of the deformation amplitude. The

Wohler's curves ( $S-N_r$ ) appear as pseudo-hyperboles whose horizontal asymptote allows definition of an endurance limit corresponding to the stress amplitude ( $S_{EL}$ ), below which no fatigue failure must occur for reasonably large numbers of cycles, typically  $10^7-10^8$ .

### 3.3.2. Influence of the fatigue mode

Both fatigue modes were compared for PEI and EPO. The corresponding endurance limits were: in the case of ABM:  $S_{EL} = 24$  MPa (PEI), 28 MPa (EPO),

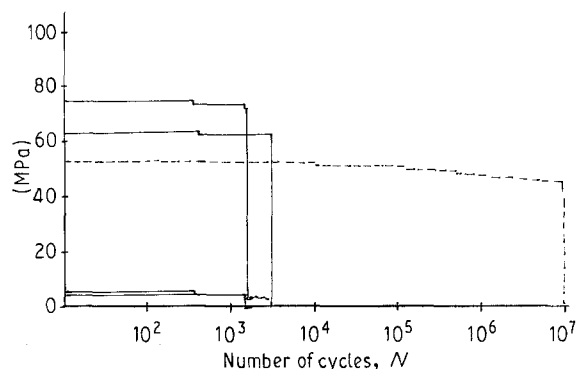


Figure 2 Examples of  $S-N$  curves for an EPO sample.

65 MPa (PEEK); in the case of OBM:  $S_{EL} = 38$  MPa (PEI), 47 MPa (EPO). The damaging rate thus appears higher for the symmetric (ABM) than for the asymmetric (OBM) loading mode.

### 3.3.3. Influence of processing conditions (for linear polymers)

SN curves corresponding to PSU and PEI are presented, respectively, in Figs 3 and 4. A detailed study of processing effects on the fatigue of these polymers will be published elsewhere; however, it must be observed that in both cases, the injection-moulded samples (strained in the melt-flow direction), have a higher  $S_{EL}$  than the compression-moulded ones. The difference is, however, considerably higher for PSU than for PEI.

### 3.3.4. Influence of polymer structure

Typical  $S-N_r$  curves of EPO, PSU, PEI and PEEK are superimposed in Fig. 5. For linear polymers, the fatigue characteristics can vary with the processing conditions, as shown above; however, the  $S_{EL}$  values are always in the following order (for ABM loading

TABLE III Mechanical static properties of the polymers under study (compression-moulded samples)

	PSU	PEI	PEEK	EPO
Specific mass ( $\text{kg m}^{-3}$ )	1242	1278	1284	1287
Packing density, $\rho^{*a}$	0.648	0.656	0.655	0.690
$T_g$ (K) <sup>b</sup>	463	493	416	483
$E$ (GPa) <sup>c</sup>	3.1	3.8	—	4.8
$M_c$ ( $\text{g mol}^{-1}$ ) <sup>d</sup>	$\approx 10^4$	$\approx 10^4$	—	193
Nature of cross-links <sup>e</sup>	Entanglements	Entanglements	Crystals	Covalent bonds

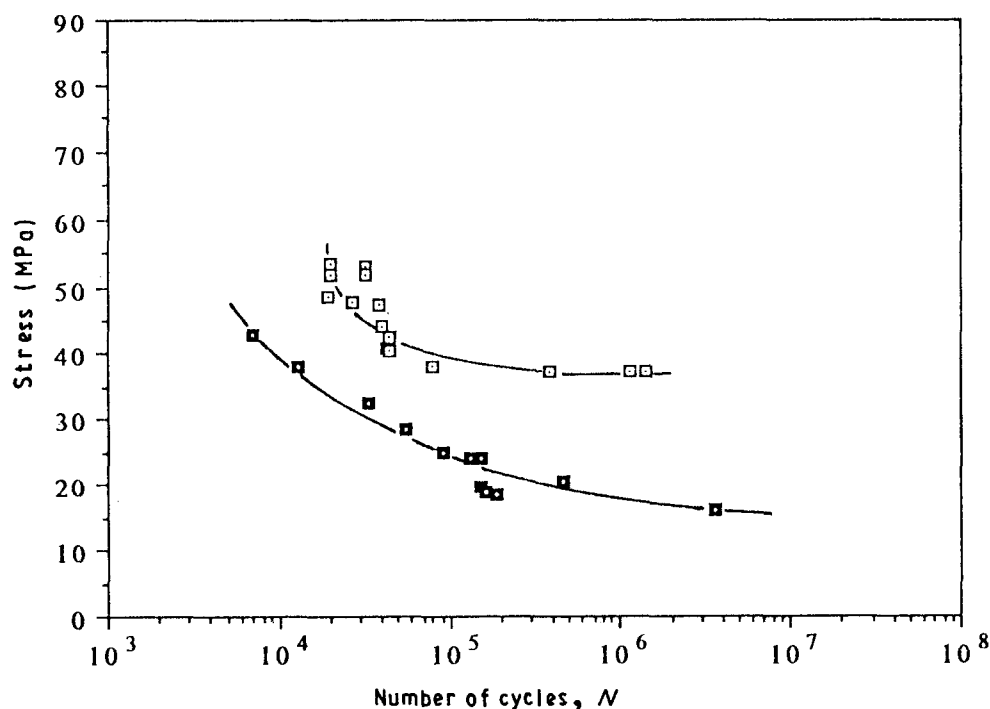


Figure 3  $S-N$  curves for (■) compression-moulded and (□) injection-moulded PSU samples in alternate bending mode. 5 Hz, 21 °C, 50% HR, zone 3.

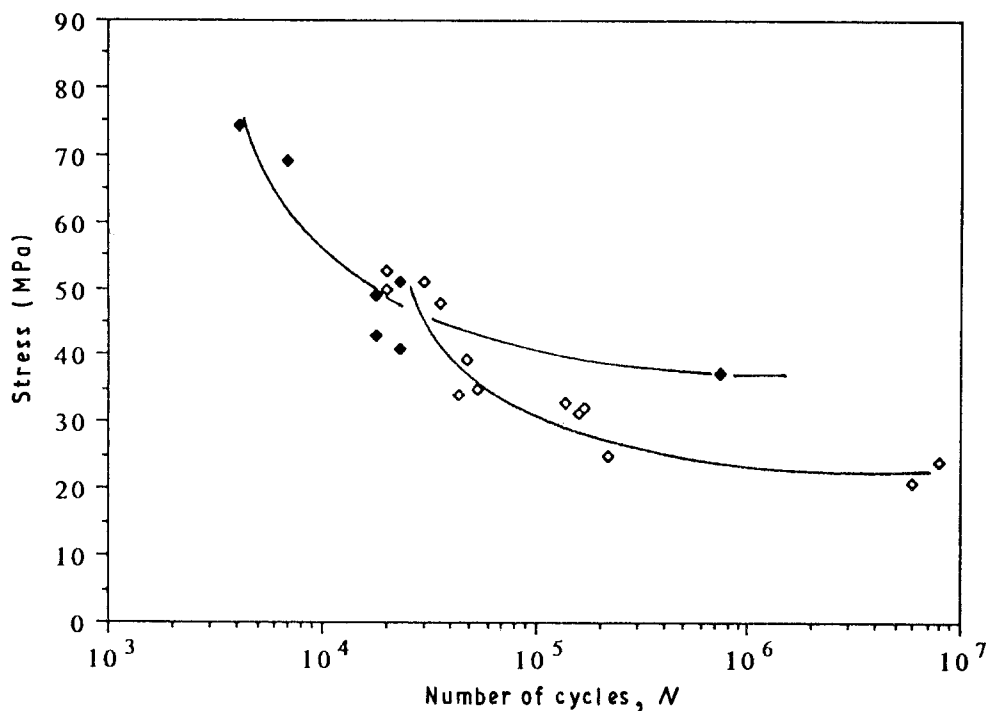


Figure 4 S-N curves for compression-moulded and injection-moulded PEI samples in alternate bending mode. ( $\diamond$ ) PEI, compression/alternate; ( $\blacklozenge$ ) PEI, compression/undulating, 5 Hz, 21 °C, 50% HR.

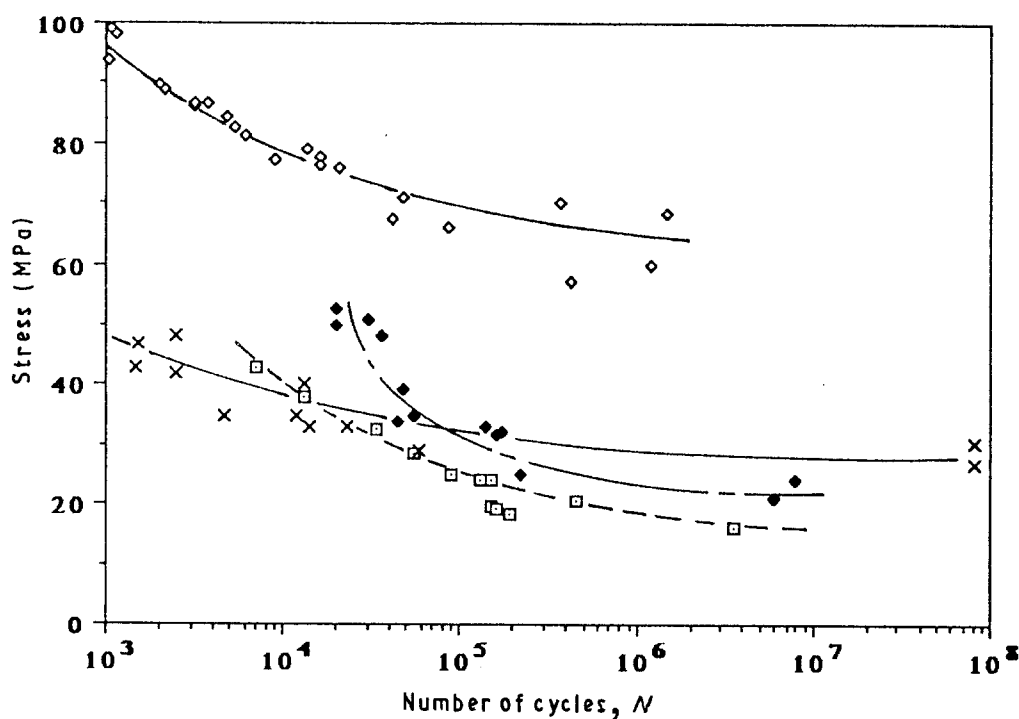


Figure 5 S-N curves in alternate bending mode for ( $\times$ ) EPO, ( $\square$ ) PSU, ( $\blacklozenge$ ) PEI and ( $\diamond$ ) PEEK. The curves correspond to injection-moulded samples for PSU, PEI and PEEK.

mode): PEEK > EPO > PSU and PEI. Some characteristic  $S_{EL}$  values are listed in Table IV.

#### 4. Discussion

##### 4.1. Static properties

The data obtained from static testing reveal clearly the higher ductility of thermoplastics compared to the thermoset under study. It is often assumed that the rupture properties depend directly on the network

structure [17, 18]. In fact, in principle, the end-to-end distance of a chain is proportional to the square root of the molar mass between entanglements ( $M_c$ ) in a random coil, and to  $M_c$  in its extended form, so that the maximum extensibility of a network must be proportional to  $M_c^{1/2}$ , i.e. must decrease with the crosslink density. Indeed, depending on the network architecture, stress concentrations must occur in certain network junctions [19] and lead to failure at deformation levels lower than predicted ones.

TABLE IV Comparison of fatigue endurance limits, ( $S_{EL}$ ), and crack propagation characteristics,  $K_{Ic}$ ,  $G_{Ic}$

Polymer	Processing	$G_{Ic}$ ( $J m^{-2}$ )	$K_{Ic}$ ( $MPa m^{1/2}$ )	$S_{EL}$ (ABM) (MPa)
PSU	Comp. moulding	5000	3.54	18
PSU	Inj. moulding	4400	3.5	39
PEI	Comp. moulding	2050	2.93	24
PEI	Inj. moulding	2060	2.9	29
PEEK	Inj. moulding	10000	6	65
EPO	Cast. moulding	110	0.6	28
PC	Inj. moulding	3750	3	–

Despite that, certain epoxy networks of high cross-link density with  $M_c$  values of the same order of magnitude as the EPO system under study ( $M_c \approx 200 \text{ g mol}^{-1}$ ), display a ductile behaviour characterized, for instance, by tensile ultimate elongation and  $G_{Ic}$  values of, respectively, 50%–100% and  $\approx 1000 \text{ J m}^{-2}$  [20]. In fact, all these systems have a relatively low glass transition temperature ( $T_g \leq 120^\circ\text{C}$ ). According to the free-volume theory [21], yielding and plastic deformation responsible for high  $G_{Ic}$  values [22], must occur at stress levels as low as  $T_g$  decreases, and then become more and more competitive with fracture mechanisms responsible for brittleness. For these systems of low  $T_g$ , capable of undergoing relatively large plastic deformations, it is reasonable to suppose that the network structure controls the fracture properties. In the case of thermosets formed of stiff subchains, characterized by high  $T_g$  values, the theoretical yield stress predicted from free-volume considerations, is very high and deformation mechanisms leading to brittle rupture become highly competitive, which can explain the lower  $\epsilon_r$  and  $G_{Ic}$  values observed for EPO. It remains to be explained why yielding is allowed for linear polymers of high  $T_g$  values such as PEI and PSU. Consideration of Poisson's ratio, directly involved on stress-induced free-volume creation [21], or of activation volume of the  $T_g$ –stress relationship, as proposed by Chow [23] could account for the difference between these polymers and EPO. Unfortunately, most of the basic physical data needed to verify these assumptions is yet lacking.

#### 4.2. Fatigue properties

All the observed ruptures are of the brittle type: as soon as a crack is initiated, it propagates almost instantaneously through the whole sample thickness. The fact that the alternate bending mode leads to shorter lifetimes than the undulating bending mode can be interpreted as follows: both fatigue modes differ essentially by the fact that compressive forces developed in the concave part of deformed samples are considerably higher in the case of ABM than in the case of UBM. Their role in damage creation is, presumably, more important than the role of cumulative creep effects of tensile stresses.

For linear amorphous polymers PEI and PSU, the influence of processing conditions reveals the positive

effect of macromolecular orientation on the fatigue lifetime. Other factors, such as the presence of defects (microvoids) or internal stresses, will be analysed elsewhere, but seem to have a second-order influence relative to orientation, at least in the absence of macrodefects such as welding lines, whose influence is well established in the case of polycarbonate [11]. This influence was also observed for PEI in a preliminary study of the fatigue of samples differing in some detail of the mould-cavity configuration [24].

The difference between PEI and PSU could be interpreted in a similar way to that of Takemori *et al.* [25] for epsilon-shaped cracking. According to these authors, this latter damaging mechanism appears when shear flow becomes competitive relative to crazing or breakdown. This leads to determination of a criterion:  $\epsilon_c/\sigma_y$  ( $\epsilon_c$  being the critical strain for crazing and  $\sigma_y$  the yield stress). The study of 12 polymers shows that epsilon cracks appear for high values of  $\epsilon_c/\sigma_y$ , typically higher than  $0.3\text{--}0.4 \text{ GPa}^{-1}$ . They are not observed for PSU and PEI, but the former is in the “transition” zone ( $\epsilon_c/\sigma_y = 0.36$ ), whereas the latter is clearly in the family of polymers giving no epsilon crazing ( $\epsilon_c/\sigma_y = 0.22$ ). Indeed, orientation must modify  $\epsilon_c/\sigma_y$ ; it is well known that it does not favour crazing. Thus, it could be supposed that isotropic (compression-moulded) PSU is in the family of epsilon-crack-forming polymers whereas oriented (injection-moulded) PSU and PEI (whatever its processing mode), are in the other family, which would be at least qualitatively consistent with the results of  $S_{EL}$  measurements. Indeed, a direct transposition of Takemori's data to the cases under study would be abusive, due to the difference in loading conditions (compressive damaging does not occur in Takemori *et al.*'s case [25], but the approach seems to be valid.

The most interesting result of this study concerns, without doubt, the influence of polymer structure, as illustrated by Fig. 5 and Table IV. The fatigue lifetimes obtained at high stress levels (typically stress amplitudes higher than 30 MPa, are greater for thermoplastics than for the thermoset, which is consistent with the static testing data. For low stress levels, however, the opposite trends are observed, at least for amorphous polymers, and the endurance limit appears to be independent of ductility or toughness, as defined from static tests. In other words, the nucleation of microdefects is not under the control of the same structural parameters as is crack propagation.

The order of magnitude of strains near to the  $S_{EL}$  is about 1%. In this domain, it is generally recognized that the behaviour essentially depends on short-scale (molecular) rather than large-scale (macromolecular and morphological) structure for glassy polymers. Among short-scale structural parameters, hydrogen bonding could explain the difference between EPO and linear polymers. For brittle rupture, a simple proportional relationship must exist between ultimate stress and cohesive energy density [26] as a result of the basic principle of linear elastic fracture mechanics. However, despite the relatively high strain rate ( $0.17 \text{ s}^{-1}$ ) of fatigue tests, viscoelastic effects cannot be ignored. At this frequency, all the polymers are (at

20°C) far above their beta transition, so that local motions can also be involved in defect nucleation [27]. From this viewpoint, all the amorphous polymers under study display a relatively intense beta dissipation peak in their viscoelastic spectra (compared, for instance, to cross-linked polyesters, polystyrene or PMMA).

From a comparison of ultrasonic and quasi static modulus measurements (Tables II and III), it appears that the beta transition remains below the ambient temperature at 5 Mz frequency for PEI and PSU, but is close to this temperature for EPO. The hypothesis of a role of the large-scale structure should, however, be considered. In fact, it is interesting to note that, as quoted in the introduction, semi-crystalline polymers are generally more fatigue resistant than amorphous ones. They have, in common with the thermosets, the existence of a network structure, the crystals being considered as physical cross-links.

A possible role of cross-linking consists in reducing the gap between the coiled and extended macromolecular configurations, whose importance is crucial in phenomena such as crazing. This gap is also reduced by macromolecular orientation because it is well known that orientation improves the resistance to crazing in brittle polymers such as polystyrene. All the results reported here would thus be consistent with the hypothesis of a stabilizing role of cross-linking on fatigue crack nucleation. This latter would occur through a mechanism involving a large-scale configurational change, eventually competitive with homogeneous shear flow. In this case, Takemori *et al.*'s approach [25], eventually modified to take into account the specificity of loading mode (existence or not of compressive stresses, for instance), could be tentatively used to predict  $S_{EL}$  values. Unfortunately, the very few available experimental data on the fatigue of cross-linked polymers in the glassy state do not allow us to establish definitely the structure-properties relationships in this field.

## 5. Conclusion

Physical (by crystallites) or chemical cross-linking inhibits or reduces the transition between coiled and extended-chain configurations which could be responsible for crack initiation. Because the latter governs largely the fatigue lifetime of the polymers under study, at least for moderate to low stress levels, it appears that ductility and toughness, which presumably play a key role in crack propagation, have practically no influence on the fatigue durability in the conditions under study. The use of a criterion such as critical strain/yield stress for damage, adapted to the chosen loading mode, can be envisaged.

## Acknowledgements

This work was sponsored by the Direction des Etudes et Recherches, Division Matériaux, which is gratefully

acknowledged. Special thanks to Dr Bellenger for ultrasonic measurements.

## References

1. V. P. TAMUSZ and V. S. KUKSENKO, "Fracture micro-mechanics of polymer materials" (Martinus Nijhoff, La Haye, 1981).
2. R. W. HERZBERG and J. A. MANSON, "Fatigue of Engineering Plastics" (Academic Press, New York, 1980).
3. C. B. BUCKNALL, K. J. GOTHAM and P. J. VINCENT, in "Polymer Science", edited by A. D. Jenkins (North Holland, London, 1972) Ch. 10.
4. Proceedings of the PRI International Conference, "Fatigue in Polymers" ed C. D. Bucknall (Plastics and Rubbers Institute, London, 1983).
5. A. MOET, in "Failure of Plastics", edited by V. Brostow and R. D. Corneliussen (SPE Hanser, New York, 1986) Ch. 18, pp. 345-56.
6. A. J. KINLOCH and R. J. YOUNG, "Fracture behavior of polymers" (Applied Science, London, 1983).
7. J. P. TROTIGNON and J. VERDU, *J. Appl. Polym. Sci.* **34** (1987) 19.
8. K. V. GOTHAM and M. C. HOUGH, RAPRA Report, "The durability of high temperature thermoplastics" (RAPRA, Shrewsbury, 1989).
9. M. T. TAKEMORI and D. S. MATSUMOTO, *J. Polym. Sci. Polym. Phys. Ed.* **20** (1982) 2027.
10. D. S. MATSUMOTO and M. T. TAKEMORI, *Polymer Commun.* **24** (1983) 41.
11. R. BOUKHILLI, R. GAUVIN and M. GOSSELIN, "Fatigue behavior of injection molded polycarbonate and polystyrene containing weld lines". 47th SPE Annual Technical Conference, NY (1989) pp. 1566-70.
12. J. P. TROTIGNON, E. MOREL and J. VERDU, *J. Mater. Sci. Lett.* **10** (1991) 844.
13. R. GAUVIN and J. P. TROTIGNON, *J. Test. Eval. ASTM* **6** (1978) 48.
14. E. MOREL, V. BELLENGER, M. BOCQUET and J. VERDU, *J. Mater. Sci.* **24** (1989) 69.
15. V. BELLENGER, W. DHAOUI, E. MOREL and J. VERDU, *J. Appl. Polym. Sci.* **35** (1988) 563.
16. J. VERDU, V. BELLENGER and E. MOREL, in "Development and Design with Advanced Materials", edited by G. C. Sih, S. V. Hoa and J. T. Pindera (Elsevier, Amsterdam, 1990) Ch. V, pp. 249-56.
17. S. WU, *Polym. Engng Sci.* **30** (1990) 753.
18. J. D. LEMAY, B. J. SWETLIN and F. N. KELLY, *Amer. Chem. Soc.* **10** (1984) 165.
19. R. J. MORGAN, *Adv. Polym. Sci.* **72** (1985) 1.
20. T. D. CHANG and J. O. BRITAIN, *Polym. Engng Sci.* **22** (1982) 1228.
21. J. D. FERRY and R. A. STRATTON, *Kolloid Z.* **171** (1960) 107.
22. K. J. PASCOE, in "Failure of Plastics", edited by W. Brostow and R. D. Corneliussen (Hanser, Munich, 1986) Ch. 7, p. 119.
23. T. S. CHOW, *Polym. Engng Sci.* **24** (1984) 1079.
24. J. P. TROTIGNON, unpublished results, 1991.
25. M. T. TAKEMORI, R. P. KAMBOUR and D. S. MATSUMOTO, *Polym. Commun.* **24** (1983) 297.
26. J. L. GARDON, *J. Colloid Interface Sci.* **59** (1977) 582.
27. B. ESCAIG, *Polym. Engng Sci.* **24** (1984) 737.
28. A. J. KINLOCH, *Adv. Polym. Sci.* **72** (1985) 45.

Received 2 January

and accepted 2 September 1992